BOLETIN DEL INSTITUTO DE TONANTZINTLA, Vol. 2, No. 3, Diciembre 1977

S P E C T R O S C O P Y O F S H O R T P U L S E S

Chandrasekhar Roychoudhuri and Sergio Calixto

SUMARIO

En este artículo presentamos un análisis general y elemental para espectroscopía de pulsos cortos usando instrumentos por interferencia de dos y múltiples haces. Las modificaciones de las franjas de interferencia son debidas a las propiedades del instrumento, al tamaño finito del pulso y a las frecuencias que componen al pulso (espectro). Así la determinación del espectro de un pulso requiere el conocimiento de la forma del pulso y las propiedades del instrumento como replicador del pulso.

ABSTRACT

We present a generalized but an elementary analysis for short pulse spectroscopy using two-beam and multiple-beam interference instruments. The various modulations of the interference fringes are due to the properties of the instrument, the finite size of the pulse and the carrier frequencies (spectrum) of the pulse. So the determination of the spectrum of a pulse requires a knowledge of the pulse shape and the properties of the instrument as a pulse replicator.

I. *Introduction*

We define spectroscopy of electromagnetic radiations as the objective to determine the high frequency at which the incident radiation oscillates. In general, the radiation may go through various modulations like amplitude, phase and frequency. Here we shall consider only the amplitude modulation of the radiation and we will represent our signal as $V(t) \exp(2\pi i\nu t)$, where $V(t)$ (a real function) is the amplitude envelope of the radiation that is oscillating at a frequency ν. Our objective is to find out ν. In the low frequency radio range, this objective can be simply achieved by using a sharply tuned oscillator or a simple galvanometer for extremely low frequency oscillations; of course, the envelope function should be slowly varying compared to the frequency of oscillation. But for extremely high frequency electromagnetic radiation, we do not as yet have any amplitude detectors to take readings; we have only square law detectors. We cannot measure the frequency of oscillation directly. The solution is to use the phenomenon of interference to our advantage. If the incident signal is superposed with a reference signal (or a part of itself) containing known parameters, then a square law detector could indirectly give the frequency of the signal through the time varying beat signals due to interference. This is the essential principle behind heterodyne (homodyne) spectroscopy (Cummins and Swinney 1970). The alternative is the older classical method of replicating the very incident signal by amplitude division (Michelson, Fabry-Perot, Lummer-Gehrcke, etc.) or by wavefront division (various gratings), and then superposing them with a time (phase) delay. The square modulus of the superposed signals while detected by a slow detector like a photographic plate can give the frequency information (Born and Wolf 1975). In this paper we shall consider such interferometric techniques of spectroscopy for pulsed light. The other known alternative method of classical spectroscopy, that we will not discuss here, is to use refractive dispersion (prism or its equivalent) to spatially separate energies due to different frequencies. But the resolving power of this method is rather limited due to the small size of prisms, although some new possibilities with gradient index fibres have been recently investigated (Cervantes 1976).

II. *Two-Beam Spectroscopy*

Suppose we have an instrument (like Michelson interferometer) that replicates two identical signals from a single incident one with a time delay of τ. The time impulse response of the instrument is,

$$H(t) = \delta(t) + \delta(t + \tau). \tag{1}$$

Then an incident signal $V(t) \exp(2\pi i\nu_0 t)$ will produce a time response,

$$\begin{aligned} B(t) &= H(t) \oplus V(t) \exp(2\pi i\nu_0 t) \\ &= V(t) \exp 2\pi i\nu_0 t + V(t + \tau) \exp 2\pi i\nu_0 (t + \tau) \end{aligned} \tag{2}$$

It is tacitly assumed that the geometry of the instrument is such that it attempts to superpose the replicated signals linearly (otherwise the above mathematical expression of linear superposition would

not be valid). Any lack of superposition will then be due to the finite size of the incident pulse. We could have written the last step of Eq. 2 directly; physically it is more appealing than first using Eq. 1 and then doing the convolution of the first step of Eq. 2. Further, since our interest is to look at the time evolving interference pattern, we shall analyze Eq. 2 directly rather than first taking its Fourier transform and then doing the inverse transform as is customarily done.

Now, suppose we have an incident pulse V (t) of width δt that is much shorter than the time delay τ. Then we would not have any superposition of the replicated pulse in Eq. 2 and the detected irradiance will be,

$$|B(t;\ \delta t \ll \tau)|^2 = V^2(t) + V^2(t+\tau), \tag{3}$$

which contains no interference term and hence there is no possibility of obtaining spectroscopic information. The other extreme case is if V (t) is unity and extends over all time. The irradiance pattern now depends only on the path delay (equivalent to a phase delay),

$$\begin{aligned} |B(\delta t = \infty)|^2 = \infty|^2 &= |\exp\ (2\pi i \nu_0 t)\ [1 + \exp\ (2\pi i \nu_0 \tau)]|^2 \\ &= 2\,(1 + \cos\ 2\pi i \nu_0 \tau). \end{aligned} \tag{4}$$

Now a straightforward counting of the fringes while varying τ will reveal the frequency of the radiation,

$$\nu_0\,(\tau_1 - \tau_2) = m\ \ (\text{no. of fringes}). \tag{5}$$

But if there are many non-coherent but continuous frequencies simultaneously present with a normalized intensity distribution F (v),

$$\int_0^\infty F(\nu)\ d\nu = 1, \tag{6}$$

then the resultant irradiance is given by Eq. 4 but integrated over all frequencies

$$|B(\nu;\ \delta t = \infty)|^2 \equiv I(\nu) = 1 + \int_0^\infty F(\nu)\ \cos\ 2\pi\nu\tau\ d\nu, \tag{7}$$

where we have absorbed the constant factor 2 in the left-hand side. Identifying the mathematical structure of this equation with the Fourier theorem, we can state that our interferogram is the Fourier transform of the spectral density function superposed over a constant background. The origin of this Fourier transform-like structure is due to the following facts. We sum over the intensities due to the frequencies F (v); the effect of mutual interference between different frequencies are negligible. Second, the interference fringes have the cosine form because they are due to the superposition of two amplitudes of the same frequency and further, the cosine form is also due to the fact that the oscillation of the radiation is considered to be sinusoidal. Now, the origin of the Fourier transform spectroscopy is immediately evident from Eq. 7. Considering only the oscillatory part,

$$I_{0s}(\nu) = \int_0^\infty F(\nu)\ \cos\ 2\pi\nu\tau\ d\nu, \tag{8}$$

one can easily find out F (v), with the help of a computer, by doing a cosine Fourier transform of the oscillatory part of the recorded interferogram (Klein 1970, Born and Wolf 1975). In the most general case of F (v), Eq. 7 can be written as (Klein 1970),

$$I(\nu) = 1 + U(\tau)\ \cos\ [2\pi\nu_0\tau + \Phi(\tau)], \tag{9}$$

where U (τ) and Φ (τ) are slowly varying functions for a narrow bandwidth F (v) compared to the high frequency cosine fringes; ν_0 is the central frequency of F (v). For the case of a symmetric F (v), Φ (τ) is zero and a simple fringe counting will give us the central frequency ν_0. But such a conclusion will

be difficult for an asymmetric spectrum because of the lack of knowledge about $\Phi(\tau)$. In any case, the visibility of the fringes (after Michelson) of Eq. 9 is,

$$V = \frac{I_{max} - I_{min}}{I_{max} + I_{min}} = U(\tau) \tag{10}$$

The Equations 4-10 have been derived on the assumption that the radiation consists of continuous oscillations. Non-interference between different frequencies were due to random phase fluctuations of the individual radiations like in a continuous wave (cw) laser running in many independent longitudinal modes.

Let us now come back to the case of more interest to us where the width δt of the pulse $V(t)$ is of the order of the delay time τ. We have a single incident pulse with a single carrier frequency and they are partially superposed. The instantaneous intensity is given by,

$$\begin{aligned} I(t, \tau) &= |V(t) \exp(2\pi i \nu_0 t) + V(t + \tau) \exp 2\pi i \nu_0 (t + \tau)|^2 \\ &= V^2(t) + V^2(t + \tau) + 2\, V(t)\, V(t + \tau) \cos 2\pi \nu_0 \tau \end{aligned} \tag{11}$$

If we use an integrating detector like a simple photographic plate exposed to the entire sequence of pulses, the total intensity is,

$$I(\tau) = \int_0^\infty V^2(t)\, dt + \int_0^\infty V^2(t + \tau)\, dt + 2 \cos 2\pi \nu_0 \tau \int_0^\infty V(t)\, V(t + \tau)\, dt, \tag{12}$$

where the first two integrals represent the same total energy due to the pulse and the last integral represents the correlation of the pulse,

$$\Gamma(\tau) = \int_0^\infty V(t)\, V(t + \tau)\, dt. \tag{13}$$

Or, by normalizing,

$$\gamma(\tau) = \frac{\int_0^\infty V(t)\, V(t + \tau)\, dt}{\left[\int_0^\infty V^2(t)\, dt\right]^{1/2} \left[\int_0^\infty V^2(t + \tau)\, dt\right]^{1/2}}. \tag{14}$$

Then the normalization of the Eq. 12 and subsequent use of Eq. 14 gives,

$$i(\tau) = 1 + \gamma(\tau) \cos 2\pi \nu_0 \tau. \tag{15}$$

So the integrated interferogram, due to a single pulse carrying a single frequency, will have a fringe modulation (visibility) given by the normalized auto-correlation of the pulse. Determination of this fringe modulation function will give us the pulse shape and, as before, the fringe counting (Eq. 5) will give us the value of the carrier frequency. We should not interpret $\gamma(\tau)$ as due to the presence of more than one frequency.

As a comment, we would like to mention that the width of a pulse carrying single frequency can be easily measured by using holography. One can record a hologram of an object of sufficient depth ($> c\, \delta t$) with the help of the pulse and then reconstruct it with a cw beam. The brightness variation of the reconstructed object will give $\gamma^2(\tau)$.

We now consider the case of a very large number of identical pulses of same carrier frequency but of arbitrary time origin and phase factor, i. e.,

$$V(t) = \sum_{n=1}^{N} V_n(t - t_n) \exp\left[2\pi i \nu_0 (t - t_n) + i\, O_n\right], \tag{16}$$

where V (t) is now a complex quantity. Then substitution of Eq. 16 in Eq. 12 reproduces the same equation for one pulse multiplied by the total number of pulses N. This can be shown by elementary algebra using the fact that the interpulse interference reduces to zero over a long time. Under this condition, the Eq. 15 for a single pulse is also valid for multitude of similar but random pulses. If the pulses, although similar in shape, contain different carrier frequencies with a spectral distribution function F (ν), then the interferogram of Eq. 15 modifies to an integral,

$$\begin{aligned} i(\tau) &= 1 + \gamma(\tau) \int_0^\infty F(\nu) \cos 2\pi\nu\tau \, d\nu \\ &= 1 + \gamma(\tau)\, U(\tau) \cos [2\pi\nu_0\tau + \Phi(\tau)], \end{aligned} \tag{17}$$

where we have used the concepts behind the Eqs. 6, 7 and 10. As before, counting the fringes will give a rough idea about the central frequency ν_0 when F (ν) is symmetric and $\Phi(\tau)$ is zero. Notice that the fringe modulation is now due to the product of the pulse correlation $\gamma(\tau)$ and the slowly varying part U (τ) of the Fourier transform of F (ν). So if one knows F (ν), then, in principle, one can find out the shape of atomic pulses from Eq. 17. If we consider F (ν) as the physical spectrum, then we must first divide the oscillatory part of the interferogram by $\gamma(\tau)$ before carrying out a computer Fourier transformation to find F (ν). This requires a knowledge of the pulse shape V (t) or its correlation $\gamma(\tau)$ Otherwise, we shall obtain a spectral function that is wider than the true spectrum F (ν). For example, in the first line of Eq. 17 one can represent the Fourier integral as f (τ) and then use the convolution theorem (Bracewell 1965) to write,

$$\begin{aligned} i_{0s}(\tau) &= \gamma(\tau)\, f(\tau) \\ &= \int_0^\infty [W(\nu) \otimes F(\nu)] \cos 2\pi\nu\tau \, d\nu. \end{aligned} \tag{18}$$

Thus the regular Fourier transform spectroscopy will give us a spectrum that is a convolution of the true spectrum with the Wiener-Khintchine spectrum (Mandell and Wolf 1965) W (ν) which, in turn, is the Fourier transform of the autocorrelation of the pulse. Eq. 18 can be used to find the Wiener-Khintchine spectrum (or the atomic pulse shape) when the physical spectrum F (ν) is known.

We can imagine a more complicated situation where each of the pulses with its carrier frequency has its own characteristic pulse shape. In other words, if the pulse shape is frequency dependent, the total interferogram should be represented as,

$$i(\tau) = 1 + \int_0^\infty \gamma(\tau, \nu)\, F(\nu) \cos 2\pi\nu\tau \, d\nu. \tag{19}$$

Recovery of F (ν) under such circumstances will be extremely difficult, if not impossible, without a detailed knowledge of $\gamma(\tau, \nu)$.

To illustrate our conceptual approach, we will present some computer curves of visibility for two simple examples: (i) a gaussian pulse with a single carrier frequency and (ii) a gaussian pulse with eleven independent carrier frequencies.

(i) Let us consider a gaussian pulse containing a single carrier frequency, assumed to be cut out from a stabilized single mode laser. The visibility curve $\gamma(\tau)$ is the autocorrelation of the gaussian pulse which again is a gaussian. Because, by autocorrelation theorem, $\gamma(\tau)$ is the inverse Fourier transform of the square of the Fourier transform of the pulse V (t) that is a gaussian. Thus $\gamma(\tau)$ will have a half-width which is double that of the incident pulse V (t). A computer plot of the visibility curve for a gaussian pulse V (t) of a half-width of 10 picoseconds and carrier frequency $\nu_0 = 2.7 \times 10^{14}$ Hz is shown in Fig. 1 (the full width at 1/e value is 20 psec.). The horizontal scale has been represented by the order of interference m instead of τ. The conversion factor is given by,

$$\tau = \frac{d}{c} = \frac{d/\lambda_0}{c/\lambda_0} = \frac{m}{\nu_0}, \tag{20}$$

where d is the path delay. We have plotted the curve of Fig. 1 by actually finding the visibility of the fringes at various points by a computer using the Eqs. 11 and 12, instead of directly plotting autocorrelation of the pulse. This was done for two purposes. First, we wanted to check our program for

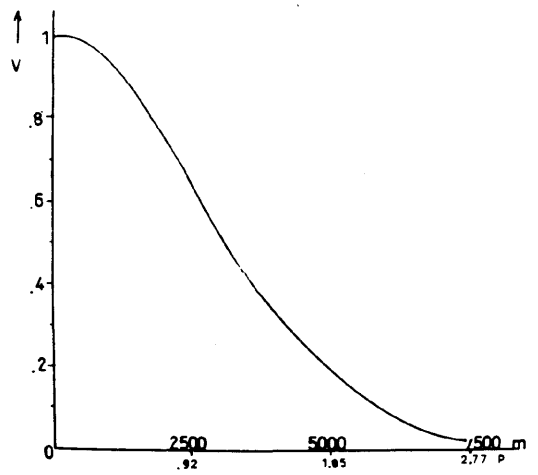

Fig. 1. *Visibility curve for two-beam interference fringes given by an integrated interferogram produced by a gaussian pulse of width* $\delta t = 10$ *picoseconds having a single carrier frequency.*

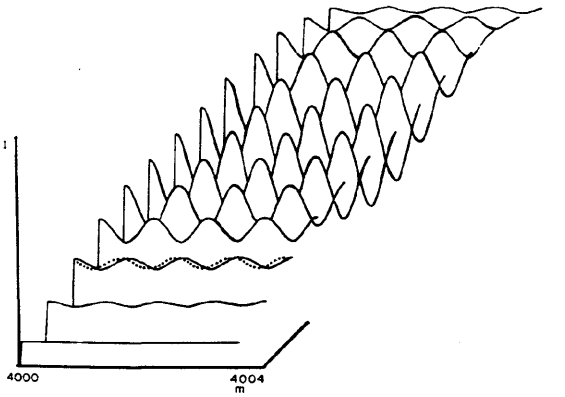

Fig. 2. *The variation in time of the visibility of two-beam cosine fringes formed by a gaussian pulse of half-width* $\delta t = 10$ *picoseconds having a single carrier frequency as it propagates through the two-beam interferometer system. The displaced dotted curve corresponds to fringes due to a different frecuency if it existed.*

N beam interference by putting $N = 2$ since the intensity due to multiple beam interference is rather complicated in terms of correlation function (Eq. 30, next section). Second, we wanted to plot the continuous irradiance variation with time to emphasize that the final visibility $\gamma(\tau)$ is actually the resultant of a time varying visibility. This is shown in Fig. 2 with a three dimensional plot for a few consecutive fringes around $m = 4000$ ($\tau = 1.48 \times 10^{-11}$ sec., half-width $= 10^{-11}$ sec.). Since the two pulses are displaced, the amplitude due to the second pulse is negligible at the tail of the beginning of the first pulse and hence, there are no fringes but a constant background. With time, as we enter into the middle of the two displaced pulses, the amplitudes are comparable and hence, we have high visibility fringes which again die out in time. The final integrated interferogram is the sum total of these time varying fringes from which the visibility curve of Fig. 1 has been plotted. Let us note the dotted curve of Fig. 2. This is the fringe position corresponding to a hypothetical frequency $\nu_0 + \delta\nu$, if it existed. This further lowers the fringe visibility of the resultant fringes. We shall consider such a case below.

(ii) Suppose the gaussian pulse of the last example has eleven carrier frequencies cut out from a *cw* laser running in eleven independent longitudinal modes. The intensities of the modes are assumed to follow a gaussian envelope (of half width $\Delta\nu = 10^{11}$ *Hz*). This is because a usual laser medium has gaussian gain envelope. Further, these eleven frequencies are concentrated around the central frequency $\nu_0 = 2.7 \times 10^{14}$ *Hz* with $\delta\nu = c/2L = (10^{11}/11)$ *Hz*, so that they lie above the laser gain threshold. Mathematically, the physical spectrum is,

$$F(\nu) \sim \sum_{n=-5}^{+5} \delta(\nu_0 + n\,\delta\nu) \exp\left[-(\nu_0 + n\,\delta\nu)^2/\Delta\nu^2\right]. \tag{21}$$

Each of these independent frequencies will have its own high frequency fringes displaced from each other by δm such that,

$$\frac{\delta m}{m} = \frac{\delta\nu}{\nu} = \frac{\delta\lambda}{\lambda}. \tag{22}$$

But the interferogram will show only the resultant fringe pattern as shown in Fig. 3a and b. The horizontal axis shows the order of interference $m_0 = \nu_0\tau$; for other frequencies the order will be different according to $m = \nu\tau$ for the same delay τ. These fringes do not show the modulation due to the pulse shape because we have chosen that particular instant to plot these fringes when the two pulses are superposed with equal amplitudes. The effect of overall modulation of the time integrated fringes by both the frequency distribution function $F(\nu)$ and the pulse correlation function $\gamma(\tau)$ is shown in Fig. 4. Notice that the visibility curve, although steadily dying according to gaus-

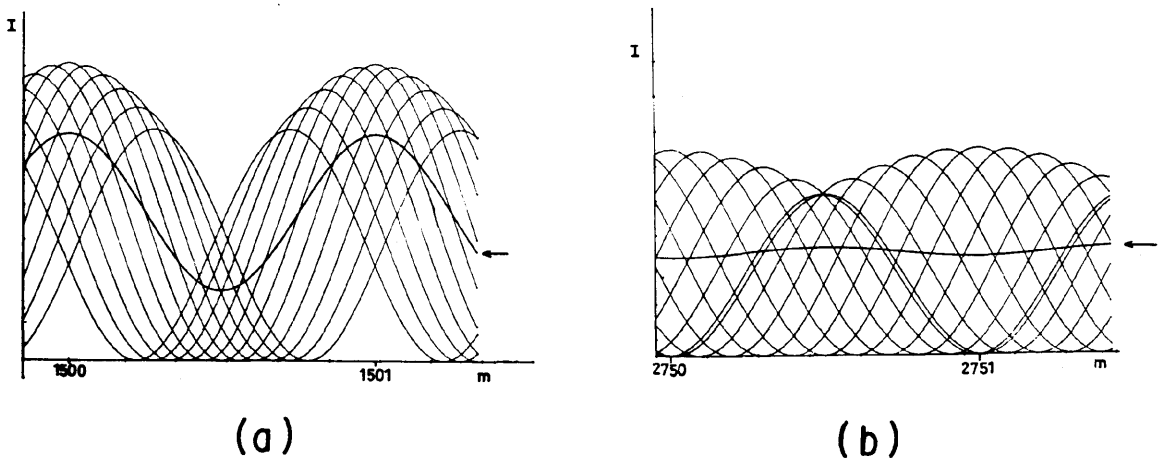

Fig. 3. *The resultant of two-beam fringe patterns due to many carrier frequencies. The fringes correspond to an instant when the two superposed pulses have equal amplitudes. a) corresponds to a delay of* $p = \tau/\delta t = .55$ *(or* $m = 1500$*), where* δt *is the half-width of the gaussian pulse. b) corresponds to* $p = 1.01$ *(or* $m = 2750$*); notice the interchange of the maxima and minima of the resultant fringe pattern compared to the case a).*

sian $\gamma(\tau)$, has secondary peaks due to the product of $\gamma(\tau)$ and the slowly varying part of the Fourier transform of $F(\nu)$ (see Eqs. 17 and 21) which is oscillatory. By comparing Fig. 4 with Fig. 1, we see the effect of the presence of different physical frequencies within the same pulse shape. Another point of interest is that visibility of the fringes after the first zero, in reality, has undergone a change in phase in the sense that the maxima and the minima have undergone a complete interchange in their position in the sequence. The reason is clearly illustrated by the resultant fringe of Fig. 3b.

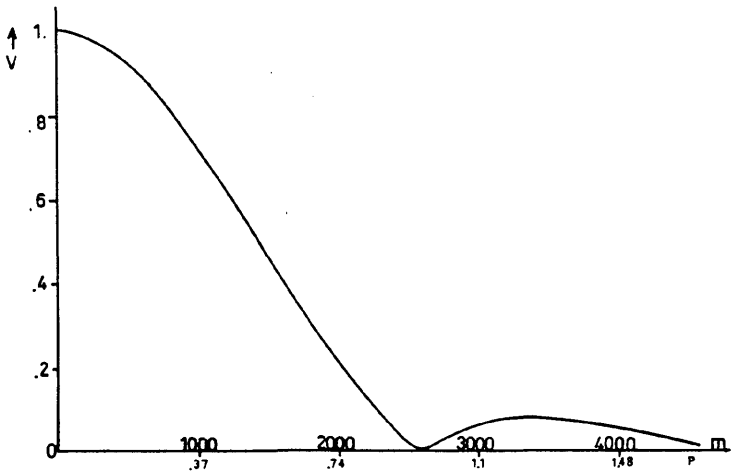

Fig. 4. *The visibility curve for two-beam interference fringes given by an integrated interferogram produced by a gaussian pulse of half-width* $\delta t = 10$ *picoseconds and carrying 11 different frequencies of oscillation with mean* $\nu_0 = 2.7 \times 10^{14}$ *Hz. In reality the visibility has changed its sign in the second peak as illustrated in Figure 3 b (see also text).*

MULTIPLE-BEAM SPECTROSCOPY

Fabry-Perot and Lummer-Gehrcke interferometers and various gratings are representative of this class of spectrometers. These instruments, either through amplitude division or through wavefront division, produce a large number of replicated waves with a common-difference path delay τ between any pair of consecutive wavefronts. When these replicated wavefronts interfere due to real physical superposition (Roychoudhuri 1975, 1977a) one can expect to obtain spectral information regarding the incident pulse. The time impulse response is given by,

$$H(t) = \sum_{n=0}^{N-1} TR^n \delta(t + n\tau), \tag{23}$$

where TR^n represents the diminution of the amplitudes in multiple reflection due to the transmission (T) and reflection (R) coefficients for Fabry-Perot and Lummer-Gehrcke interferometers; for gratings this factor is unity. N is the effective number of pulses produced by the instrument. It is limited by the number of slits for a grating, by the size of the plate (number of reflections) for a Lummer-Gehrcke plate and by the finesse number for a Fabry-Perot (higher order reflections carry very little energy ($R^n \approx 0$). For all the cases, τ is $m\lambda/c$, where m is the order for interference. An incident pulse $V(t)$ exp $(2\pi i\nu_0 t)$ will produce a time response of,

$$\begin{aligned} B(t) &= H(t) \otimes V(t) \exp 2\pi i\nu_0 t \\ &= \sum_{n=0}^{N-1} TR^n V(t + n\tau) \exp [2\pi i\nu_0 (t + n\tau)]. \end{aligned} \tag{24}$$

As in the last section (Eq. 3), if the pulse width δt is much shorter than the delay time τ, the irradiance consists of a series of time pulses with no interference whatsoever,

$$|B(t;\ \delta t \ll \tau)|^2 = \sum_{n=0}^{N-1} T^2 R^{2n} V^2(t + n\tau). \tag{25}$$

Under these circumstances, these spectrometers are totally incapable of producing any spectral information; they can only behave as pulse multiplicators (Top et al 1971, Roychoudhuri 1977b). We note here that interference spectrometers do not possess any inherent property as a spectrum analyzer; they are only pulse multiplicators. If the incident pulse is so long as to produce a superposition of N beams, then it is the property of the superposed fields to separate (disperse) their energies according to their physical frequencies. So, in general, it will be incorrect to use the Fourier transform of the response function of such an instrument to a continuous monochromatic wave as its time impulse response (Eberly and Wódkiewicz 1977). These passive instruments cannot carry out Fourier transform of pulses because it is a non-casual integral process requiring information from the past to the future (a pulse propagates through the instrument with a finite velocity; see Roychoudhuri 1976).

The second extreme case of Eq. 24 is obtained when the incident is a continuous and monochromatic one with $V(i) = 1$,

$$\begin{aligned} |B(\delta t = \infty)|^2 &= \left| \sum_{n\ 0}^{N-1} TR^n \exp [2\pi i\nu_0 (t + n\tau)] \right|^2 \\ &= T \frac{1 + F_N \sin^2 \pi N\nu_0\tau}{1 + F \sin^2 \pi\nu_0\tau} \text{ or } \frac{\sin^2 \pi N\nu_0\tau}{\sin^2 \pi\nu_0\tau}, \end{aligned} \tag{26}$$

where the first form is for a Fabry-Perot or a Lummer-Gehrcke and the second form is for a grating with $TR^n = 1$ and also,

$$\begin{aligned} T &= T^2 (1 - R^N)^2 / (1 - R)^2. \\ F_N &= 4R^N / (1 - R^N)^2. \\ F &= 4R / (1 - R)^2. \end{aligned} \tag{27}$$

For a Fabry-Perot with N as the finesse number$R^N \approx 0$; this is approximately equivalent to having an infinite sum because the last terms are effectively zero and one obtains the classical Airy formula in (26) with the numerators as unity (Born and Wolf 1975). It is important to note from Eq. 26 that even for a single frequency continuous radiation the so called spectral function has a finite width instead of a δ-function response. This is essentially because the total number of beams which are interfering is effectively limited by N. In other words, the continuous radiation has been effectively cut into a long but finite pulse by the instrument.

Let us come back to the case of our major interest, a single pulse of width δt comparable to τ and carrying a single frequency of oscillation. We have from Eq. 24,

$$I(t) = |B(t;\ \delta t \sim \tau)|^2 = \left| \sum_{n=0}^{t-1} TR^n\, V(t + n\tau) \exp\left[2\pi i \nu_0 (t + n\tau)\right] \right|^2 \qquad (28)$$

Notice that we have changed the summation limit from $(N-1)$ to $(M-1)$ where $M \leqslant N$, to emphasize that for a short pulse not all the N replicated pulses are physically superposed because of the finite size of $V(t)$ and the displacement τ.

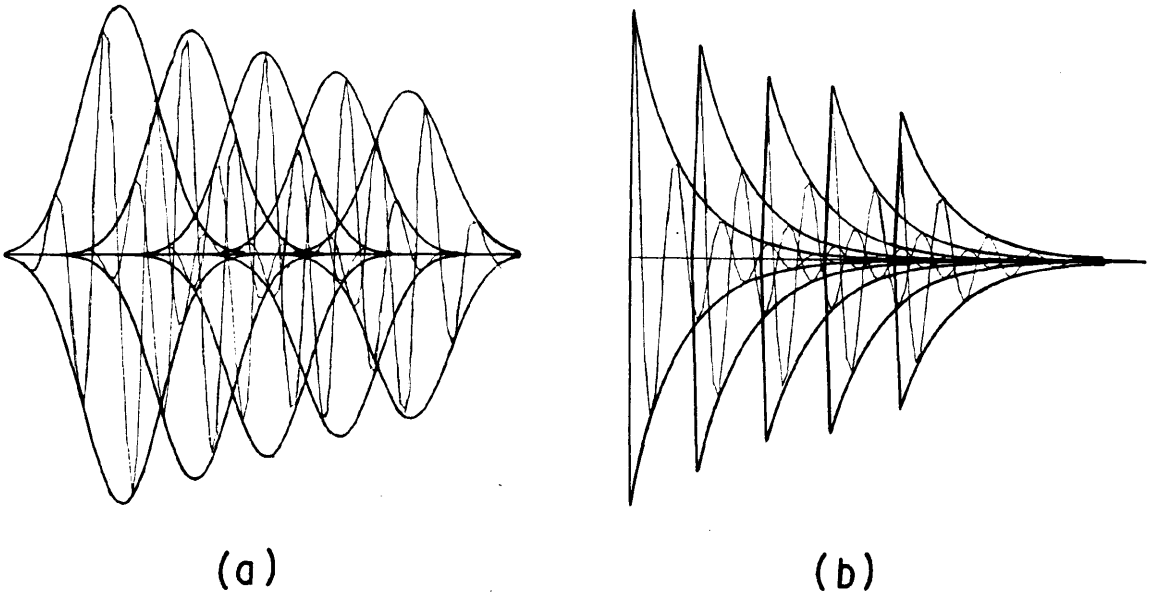

Fig. 5. *A multiple-beam interferometer replicates a single incident pulse into a train of pulses with a characteristic regular delay. If the delay is smaller than pulse width, there is partial superposition of the train of pulses. In a) we have a gaussian and in b) we have an exponential incident pulse. For illustration the carrier frequency oscillation with a rather long period has been drawn within the amplitude envelopes. The multiple-beam interferometer for this case is a Fabry- Perot (R = .9).*

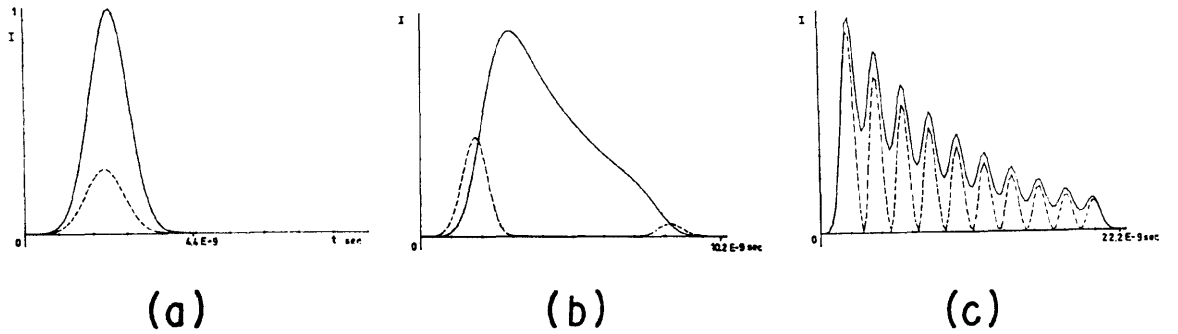

Fig. 6. *Time varying resultant intensity due to multiple-beam interference (Fabry-Perot, R = .9) produced by a gaussian pulse of width $\delta t = 1 \times 10^{-9}$ sec. with a single carrier frequency. Cases a), b) and c) correspond to three different delay times of $\tau = p\ \delta t$ where p = 0.013, 0.668, and 2.004 respectively. All the exampels have solid curves corresponding to the integral order of interference ($m_{1,2,3} = \nu\tau_{1,2,3}$ and dashed curves corresponding to immediate half-integral order of interferences ($m_{1,2,3} + 0.5$). For convenience of computation, only 10 consecutive pulses out of the entire train have been taken into account.* F

First, let us look at the various computer solutions of such a superposition. Fig. 5a and b show superposition of a train of amplitude pulses of gaussian and experimental form. The resultant irradiance pattern varies with time depending upon the delay and order of interference. This is shown in Fig. 6a, b, and c for the case of ten gaussian pulses produced by a Fabry-Perot with increasing

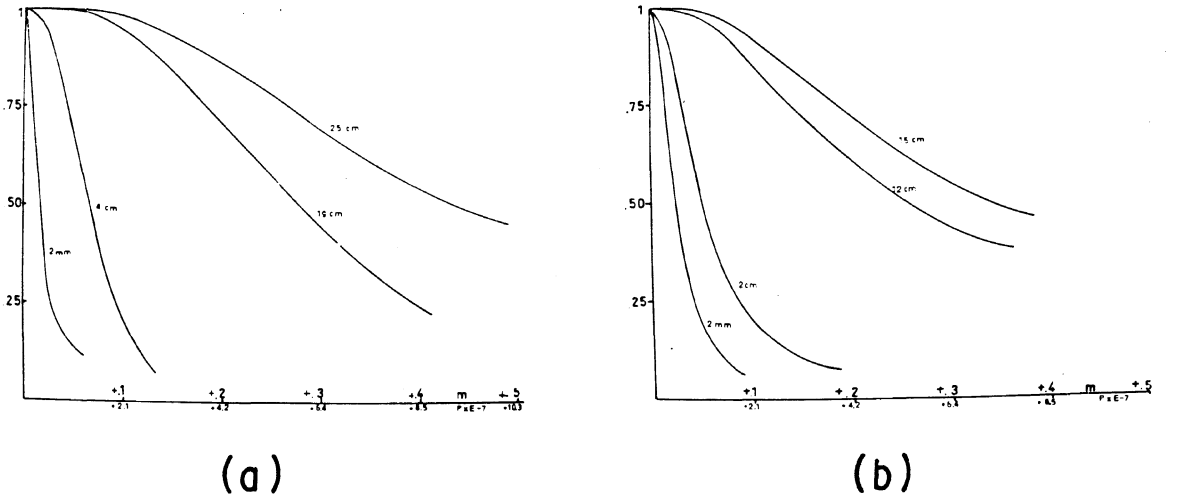

Fig. 7. *Apparent spectral response curves (of time-integrated energy distribution with change of order of interference) due to a Fabry-Perot (R = .9) produced by a single incident pulse. Curves in a) are due to a gaussian pulse of width* $\delta t = 1. \times 10^{-9}$ *seconds and those in b) are due to an exponential pulse of width* $\delta t = \sqrt{\pi}/2 \times 10^{-9}$ *seconds such that it carries equal amount of total energy as that of the gaussian pulse. Notice the increase in half-width of these apparent spectral curves with increasing delay time (plate separation in a Fabry-Perot; R = .9).*

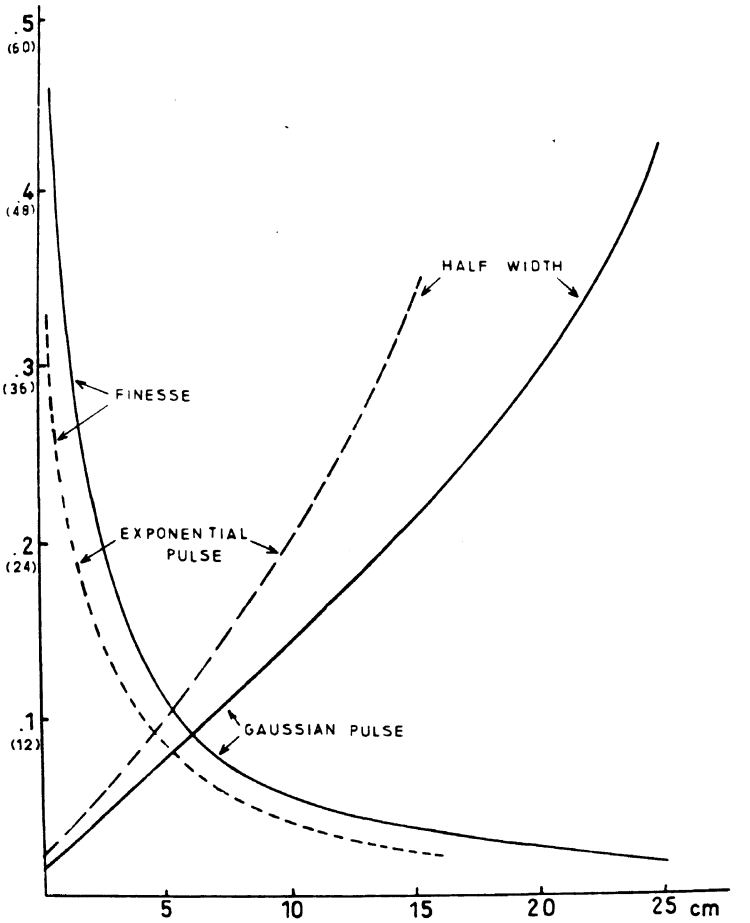

Fig. 8. *Variation of half-widths or finesses with delay time (plate separation in a Fabry-Perot; R = .9) due to a gaussian (solid curves) and an exponential (dashed-curves) incident pulse. The data are taken from multitudes of apparent spectral curves like those shown in Fig. 7.*

plate separation; each of these figures also has a lower curve (with an amplified vertical scale) to show the irradiance variation for the half-integral order of interference (destructive interference). This is the idea behind pulse shaping using Fabry-Perots (Thomas and Siebart 1972, Martin 1977) and gratings (Roychoudhuri 1977b). But one should note that these time curves (Fig. 6) will be modified for incident pulses containing more than one carrier frequency. In Fig. 7a and b we show time integrated energy variation with order of interference for a gaussian and an exponential pulse (both carrying equal amount of energy). Although each of these sets of curves show increasing half-width increasing delay between the pulses, they should not be interpreted as the existence of more than one frequency. Similar curves for rectangular pulses are shown in Roychoudhuri (1977a). In Fig. 8 we show curves for variation of half-width or finesse with increasing interpulse separation for the same gaussian (Martin 1977) and exponential pulses. Thus it is possible, at least in principle, to discern between a gaussian and an exponential pulse from their characteristic finesse variation. Detailed computer analysis of two-beam and multiple-beam spectroscopy with short pulses containing one and multiple carrier frequencies has been done by Calixto (1977).

Let us come back to Eq. 28 and simplify it algebraically.

$$I(t, \tau) = \sum_{n=0}^{M-1} T^2 R^{2n} V^2 (t + n\tau) + 2 \sum_{n<m} T^2 R^n R^m V(t + n\tau) (Vt + m\tau) \cos 2\pi\nu_0 (m - n)\tau. \tag{29}$$

If the irradiance is time integrated, for example, by a photographic plate, then using the definition of autocorrelation (Eq. 14) and absorbing the total energy $\Gamma(0)$ to the left hand side, one can write,

$$i(\tau) = \sum_{n=0}^{M-1} T^2 R^{2n} + 2 \sum_{n<m} T^2 R^{m+n} \gamma(\overline{m - n}\,\tau) \cos 2\pi\nu_0 (m - n)\tau \tag{30}$$

This is a way of presenting multiple-beam interference as the sum of many two-beam interferences. For example, with a continuous incident radiation, Eq. 26 can be rewritten as,

$$|B(\delta t = \infty)|^2 = \sum_{n=0}^{N-1} T^2 R^{2n} + 2 \sum_{n<m} T^2 R^{m+n} \cos 2\pi\nu_0 (m - n)\tau, \tag{31}$$

where, as before, factors involving T and R should be reduced to unity for a grating. Comparing Eqs. 30 and 31, we see that the fringes due to multiple-beam interference with a short pulse are modified by the pulse correlation value $\gamma(\overline{m-n}\tau)$ just as in two-beam interference (Eqs. 4 and 15). Comparing Eq. 30 with Eq. 15, we note that it is much easier to do pulse measurement or spectroscopy with a two-beam interferometer than a multiple-beam interferometer because of the involved summation of Eq. 30. Interpretation is further complicated if one has many carrier frequencies $F(\nu)$ for the same pulse,

$$i(\tau, \nu) = \sum_{n=0}^{M-1} T^2 R^{2n} + 2 \sum_{m<n} T^2 R^m R^n \gamma(\overline{m - n}\tau) \int_0^{\infty} F(\nu) \cos 2\pi\nu (m - n)\tau \, d\nu. \tag{32}$$

Then using the arguments of Eq. 17,

$$i(\tau, \nu) = \sum_{n=0}^{M-1} T^2 R^{2n} + 2 \sum_{n<m} T^2 R^m R^n \gamma(\overline{m - n}\tau) U(\overline{m - n}\tau) \cos [2\pi\nu_0 (m - n)\tau + \Phi(\overline{m - n}\tau)], \tag{33}$$

where ν_0 is the mean frequency of $F(\nu)$ and $\Phi(\tau)$ will be zero for symmetric $F(\nu)$. We again notice that, just as two-beam fringes, multiple-beam fringes are also modulated by both the pulse

correlation and the cosine Fourier transform of the spectral density function; but now the separation of the two effects is more complicated. Essentially similar Eqs. 30, 33 will be given if one has many random pulses such that mutual interferences cancel out, as we have argued following Eq. 16.

In conclusion, we emphasize the two essential points elaborated in this paper. Modulation of interference fringes takes place due to both the finite pulse size and the existence of multiple carrier frequencies. One must not interpret the combined fringe modulation as only due to carrier frequencies. Second, analysis of short pulse parameters are much easier with two-beam interferometers than with multiple-beam interferometers.

REFERENCES

Born, M. and E. Wolf, 1975, *Principles of Optics*, (Pergamon Press, New York). Ch. 7.

Bracewell, R. N., 1965, *The Fourier Transform and Its Applications* (Mc Graw-Hill, New York).

'Calixto, S., 1977, "Interpretación Espectral de Pulsos Cortos de Luz a través de la Interferencia de Dos y Más Haces", M. Sc. Thesis, Instituto Nacional de Astrofísica, Optica y Electrónica, Puebla, México.

Cervantes, M., 1976, "Espectroscopia Optica Mediante Fibras con Gradiente de Indice de Refracción", M. Sc. Thesis Instituto Nacional de Astrofísica, Optica y Electrónica, Puebla, México.

Cummins, H. Z. and H. L. Swinney, 1970, "Light Beating Spectroscopy", in *Progress in Optics*, Vol. VIII (North Holland, Amsterdam).

Eberly, J. H. and K. Wódkiewicz, 1977, "The Time-Dependent Physical Spectrum of Light", J. Opt. Soc. Am. **67**, 1252-1261.

Klein, M. V., 1970, *Optics* (John Wiley, New York); Ch. 6.

Martin, W. E., 1977, "Pulse Stretching and Spectroscopy of Subnanosecond Optical Pulses Using a Fabry-Perot Interferometer", Opt. Comm. **21**, 8-12.

Mandel, L. and E. Wolf, 1965, "Coherence Properties of Optical Fields", Rev. Mod. Phys. **37**, 231-287.

Roychoudhuri, C. 1977a, "Causality and Classical Interference and Diffraction Phenomena", Bol. Inst. Tonantzintla, Vol. 3 (this issue).

Roychoudhuri, C., 1977b, "Passive Pulse Shaping Using Delayed Superposition", Opt. Eng. **16**, 173-175.

Roychoudhuri, C., 1976, "Is Fourier Decomposition Technique Applicable to Interference Spectroscopy?", Bol. Inst. Tonantzintla **2**, 101-107.

Roychoudhuri, C., 1975, "Response of Fabry-Perot Interferometers to Light Pulses of Very Short Duration", J. Opt. Soc. Am. **65**, 1418-1426.

Top, M. R., P. M. Rentzepis and R. P. Jones, 1971, "Time Resolved Absorption Spectroscopy in the 10^{-12} sec. Range", J. Appl. Phys. **42**, 3415-3419.